공학석사 학위논문

Selective Fluoride Removal with reduced Graphene Oxide/Hydroxyapatite Composite Electrode in Electric Field Assisted System

환원 그래핀옥사이드/수산화인회석 화합물 전극을 이용한 전기장 내 선택적 불소 제거

2020 년 2 월

서울대학교 대학원

화학생물공학부

박 규 린

Abstract

Selective Fluoride Removal with reduced Graphene Oxide/Hydroxyapatite Composite Electrode in Electric Field Assisted System

Gyuleen Park

Chemical Convergence for Energy & Environment

School of Chemical and Biological Engineering

Seoul National University

Fluoride excess in drinking water is one of the most increasing concerns worldwide, causing health diseases in more than 25 countries. The number of people affected by fluoride is being estimated at about ten million, and several efforts to remove the excessive fluoride from drinking water have been carried out. For instance, there have been some research efforts to remove fluoride using capacitive deionization (CDI), which is an emerging desalination technology with an environmental-friendly and energy-efficient properties. However, those are certainly limited to the systemic studies using activated carbon (AC) electrodes, which do not have any selectivity toward fluoride. Therefore, it can lead to inefficient energy consumption for treating

fluoridated water with various ions. Hence, in this study, the reduced graphene oxide/hydroxyapatite composite (rGO/HA) was synthesized to a novel fluoride-selective electrode material using the hydroxyapatite (HA), well known as the fluoride adsorbent. As a result, fluoride was much more preferentially removed with the rGO/HA electrode having 4.9 times higher removal capacity than that of the AC electrode from ternary solution consists of fluoride, chloride, and nitrate. Through the positive relationship between the fluoride uptake and the HA content in the rGO/HA electrode, it was approved that the HA plays the main role for fluoride removal in the rGO/HA electrode. Furthermore, the rGO/HA electrode revealed the stability and reusability for the fluoride removal without significant capacity loss even after 50 cycle operation with maintaining about 0.21 mmol g^{-1} of fluoride removal capacity and 96% of regeneration efficiency. Therefore, this study suggests a novel electrode material for effective and selective fluoride removal in an electric field assisted system.

Keyword: water treatment, selective fluoride removal, reduced graphene oxide/hydroxyapatite composite electrode, electric field assisted system

Student number: 2018-20123

Contents

List of Figures

List of Tables

Chapter 1. Introduction

1.1 Research Background

As generally known, excessive fluoride in drinking water is one of the most increasing concerns worldwide, causing fluorosis in more than 25 countries (Meenakshi & Maheshwari 2006). According to World Health Organization (WHO), the permissible range of the fluoride in the drinking water is 0.5-1.5 mg L^{-1}, and over 1.5 mg L^{-1} of fluoride can give harmful impacts on human health with several fluoride related diseases (Malago 2017). For instance, immoderate fluoride in drinking water causes dental and skeletal fluorosis accompanied by severe bone deformation (Malago 2017). However, in many parts of the world like India, China, the United States, and Mexico, the fluoride concentration in the groundwater, which is the main source of the drinking water, has far exceeded the drinking water standard value (Ali et al. 2016). Thus, it is necessary to remove the excessive fluoride in the groundwater prior to the use of drinking water. In this respect, several technologies including adsorption (Meenakshi & Maheshwari 2006), ion exchange (Meenakshi & Maheshwari 2006), reverse osmosis (Meenakshi & Maheshwari 2006), and recently capacitive deionization (CDI) (Tang et al. 2015, 2016b,a) have been used to remove fluoride from water resources. Of these methods, CDI is being regarded as an upcoming technology of treating fluoride with its environmental friendliness, cost effectiveness, and energy efficiency.

CDI is an emerging desalination technology which uses porous carbon as

an electrode. It removes and releases ion species from aqueous solutions with charging and discharging step (Tang et al. 2016a). CDI system is based on the formation of an electrical double layer (EDL) within the electrode/electrolyte interface to remove unwanted ions by applying an electrical voltage difference between two porous carbon electrodes. However, despite its large surface area, the carbon electrode does not have any preference for anions and cations. This character causes consuming unnecessary charges to achieve certain ion removal performance. To remove certain ions selectively, several system developments have been investigated with ion-selective membranes (Choi et al. 2016; Kim & Choi 2010; Qian et al. 2015) or electrodes (Gan et al. 2019; Yang et al. 2013a). Recently, some systemic studies for the fluoride removal with CDI (Tang et al., 2015, Tang et al., 2016a, Tang et al., 2016b) have been employed so far. However, those were limited to the parameter studies of CDI. Furthermore, since the electrode material for the system was carbon, it was unable to achieve the selective fluoride removal.

1.2 Objectives

In this study, reduced Graphene Oxide/Hydroxyapatite composite (rGO/HA) was prepared for the fluoride-selective electrode material. Hydroxyapatite ($Ca_{10}(PO_4)_6(OH)_2$), well known as an adsorbent for fluoride removal with its low cost and high defluoridation capacity, provided the fluoride selective property for the rGO/HA electrode. The selective fluoride removal was validated with the rGO/HA electrode and compared with the conventional CDI electrode. Then the effect of the electric field on the fluoride removal performance was investigated with respect to the applied voltages. Furthermore, to evaluate the stability and reusability of the rGO/HA electrode, the fluoride adsorption/desorption capacity were estimated at initial and after the 50cycle operation of the adsorption/desorption process, respectively. Finally, the feasibility of fluoride removal in real water using the rGO/HA electrode was investigated in the real groundwater of Mukh Kampul, Cambodia.

Chapter 2. Literature Review

2.1 Fluoride Problems

2.1.1 Fluoride in drinking water

Fluoride is one of the most common contaminants in drinking water by the World Health Organization (WHO) (Bhatnagar et al. 2011), giving harmful effects on human health. Fluoride concentration under 1.5 mg L^{-1} is essential for mineralizing bones with the formation of dental enamel and even for preventing tooth decay (Meenakshi & Maheshwari 2006). However, over 1.5 mg L^{-1} of fluoride intake results in a severe bone disease, known as fluorosis. For instance, 1.5-4.0 mg L^{-1} range of fluoride intake causes dental and skeletal fluorosis, which give pain in the tooth and bones. Moreover, over 10 mg L^{-1} of fluoride concentration leads to the crippling fluorosis, which is very fatal to human health (Meenakshi & Maheshwari 2006). The main source of the drinking water is the groundwater, and the natural concentration of the fluoride in the groundwater depends on the geological, chemical and physical characteristics of the aquifer, acidity of the soil and rocks, and temperature (Meenakshi & Maheshwari 2006). Recently, excessive fluoride in groundwater is uprising for serious problems worldwide. Over 260 million people in Asia, Middle East, and Africa consume drinking water with high fluoride concentration above the WHO standard (Malago 2017) (Table 1); thus, a lot of research efforts have been carried out to treat fluoridated water.

Table 1. Countries that have fluoride problems and following range of fluoride concentration (Meenakshi & Maheshwari 2006).

Country	Range of fluoride concentration (mg L^{-1})	Reference
India	1.6-31	(Meenakshi & Maheshwari 2006)
Malawi	0.060-10	(Malago 2017)
Ethiopia	0.10-180	
Tanzania	0-140	
Algeria	0.38-2.6	(Fordyce et al. 2007)
Ukraine, Moldova	2.0-7.0	
Hungary	0.60-6.2	
Iran	1.1-4.1	(Mesdaghinia et al. 2010)
Cambodia	0.010-2.9	

2.1.2 Conventional methods for fluoride removal

Among the existing conventional methods for the fluoride removal, the adsorption is the most widely known process due to its low cost and simple design (Bhatnagar et al. 2011). Adsorbent materials such as activated alumina, activated carbon, and bone charcoal have been used for defluoridation, and especially, activated alumina and activated carbon are most commonly used (Indermitte et al. 2014) (Table 2). Adsorption process can remove fluoride up to 90%, however, it has critical limitations because it is highly dependent on pH and effectiveness decreases of the fluoride removal over the regeneration process (Meenakshi & Maheshwari 2006).

Furthermore, fluoride can be removed by the ion exchange technique. Usually, the ion exchange technique removes fluoride by adsorption rather than exchanging ions because of the comparably lower concentration of fluoride than other ions present in water (Jadhav et al. 2015). Ion exchange resin can remove fluoride up to 95%, while retaining the taste and color of water intact. However, pre-treatment is required to maintain the pH and it has regeneration and waste disposal problems due to the very low pH and high levels of chloride in the treated water (Meenakshi & Maheshwari 2006).

Precipitation and coagulation have been reported as the fluoride removal technique because of its relatively simple and cost-effective process (Oladoja & Aliu 2009). Lime ($Ca(OH)_2$, CaO, $CaCO_3$) is one of the most commonly used coagulants for the fluoride removal (Turner et al. 2005). Addition of lime leads to precipitation

of fluoride into the form of insoluble calcium fluoride (fluorite) as follows:

$Ca(OH)_{2(aq)} + 2F^-_{(aq)} \rightarrow CaF_{2(s)} + 2OH^-_{(aq)}$

However, the precipitation and coagulation process have problems that it removes only a small portion of fluoride (18-33%), and large space is required for drying sludges. Furthermore, the high maintenance costs of plants and chemicals are required (Meenakshi & Maheshwari 2006).

For the user-friendly and cost-effective technique of the fluoride removal, Reverse Osmosis (RO) membrane process has been emerged recently without posing the problems associated with the conventional methods above (Shen & Schäfer 2014). RO is a physical process in which the contaminants are removed by applying pressure on the feed water so that none of ions could pass through a semipermeable membrane. Several workers showed that it is possible to extract more than 90% of the dissolved fluoride in a single step, regardless of its initial concentration (Ndiaye et al. 2005). The process operates in a simple operating regime using a compact model with minimal manpower, and the lifetime of the membrane is also sufficiently long. Despite these advantages, it still has shortcomings because it removes all of the ions present in water, even including minerals that are essential for human health and pH correction of acidic treated water is required (Meenakshi & Maheshwari 2006). Higher costs compared to other methods, membrane fouling, and scaling also cannot be denied of the possible drawbacks of RO (Shen & Schäfer 2014).

Table 2. Well-known fluoride adsorbents and following adsorption capacity, contact time, and pH range for fluoride removal.

Adsorbent	Adsorption capacity	Contact time	pH	Reference
Hydroxyapatite	4.5 (mg g^{-1})	-	6.0	(Meenakshi & Maheshwari 2006)
Alum sludge	5.4 (mg g^{-1})	240 min	6.0	
Activated alumina (γ-Al_2O_3)	0.86 (mmol g^{-1})	16-24 h	5.0-6.0	
Activated alumina (Grade OA-25)	1.5 (mg g^{-1})	-	7.0	
Waste carbon slurry	4.3 (mg g^{-1})	1 h	7.6	
Fluorspar	1.8 (mg g^{-1})	-	6.0	
Quick lime	16 (mg g^{-1})	75 min	-	

2.2 Electrochemical Technology for Fluoride Removal

2.2.1 Capacitive deionization

Among the several techniques for ion removal, the most representative electrochemical technique is capacitive deionization (CDI). CDI has been progressed rapidly with its eco-friendliness, energy efficiency, and simple operation (Seo et al. 2010). Conventional CDI system uses one pair of oppositely placed porous carbon electrodes which store ions on the electrical double layer (EDL) (Porada et al. 2013) (Figure 1). When a potential difference is applied to the system, the cations and anions are captured onto the surfaces of the negatively and positively charged electrodes (Tang et al. 2016a). CDI operation can be separated into two consecutive steps: charging and discharging step. During the charging step, ions are stored in the electrical double layer at the surface of the electrode removing ions from the treating water. Subsequently, during the discharging step, the stored ions are released to regenerate the electrodes. In CDI, various carbonaceous materials are used for electrode materials. Among them, the activated carbon (AC) is identified to be an economically feasible option along with its simple fabrication and outstanding adsorptive performance. However, despite of its large surface area, the activated carbon does not have any preference for anions and cations. This character induces unnecessary charge consumption to achieve a certain ion removal performance; thus, it leads to various approaches to provide certain ion selectivity in CDI using ion-selective membranes (Kim & Choi 2010) and electrodes (Yang et al. 2013b).

Recently, some systemic studies for the fluoride removal in CDI have been employed in various systematic conditions such as constant current (Tang et al. 2016a) and single-pass constant-voltage (Tang et al. 2016b). In constant current operation, the feasibility of the fluoride removal was investigated by flowing the brackish groundwater continuously (single-pass mode) at both zero-volt and reverse-current desorption modes. Also, selective models were investigated to describe the selective electro-sorption with respect to fluoride and chloride (Tang et al. 2016a). With the system operated at the single-pass constant-voltage, feasibility of the fluoride removal was explored at the low-salinity groundwater, and then, the behavior of the fluoride electro-sorption was evaluated into a model (Tang et al. 2016b). However, along with the batch-mode study for the fluoride removal in CDI (Tang et al. 2015), these approaches were limited to the operation studies, which were not relevant to the enhancement of the ion removal capacity nor ion selectivity.

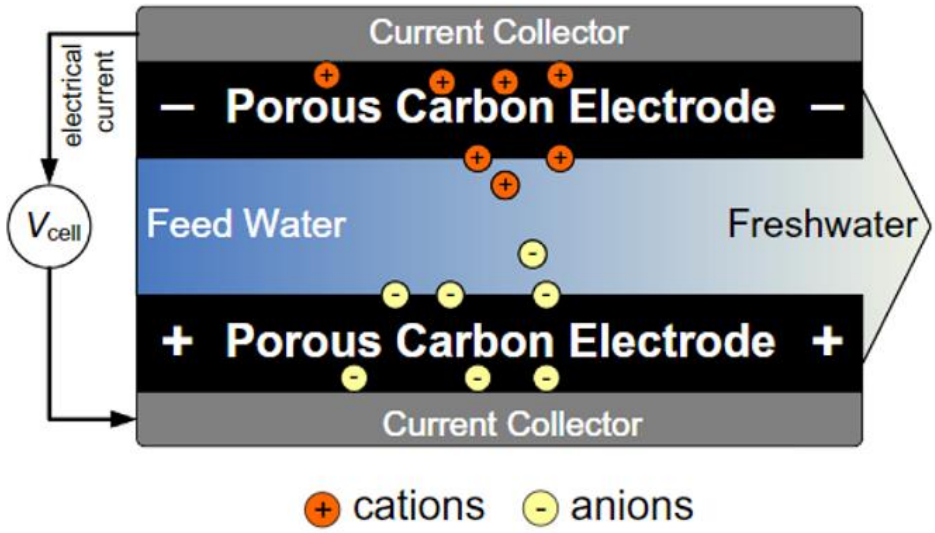

Figure 1. Schematic design of the capacitive deionization (CDI). Cations and anions are removed to the negative and positive electrodes, respectively, producing freshwater with a potential difference applying (Porada et al. 2013).

2.2.2 Electrodialysis

Electrodialysis (ED) is one of the most commercialized desalination methods for water treatment which has been used for many years. ED separates ions across charged membranes from one solution to another using the electrical potential difference as a driving force. In a typical ED system, series of anion and cation exchange membranes are arranged alternatively between an anode and cathode to form individual channels (Figure 2). When a direct current potential is applied between two electrodes, the positively charged cations move to the cathode, passing through the negatively charged cation exchange membrane and retained by the positively charged anion exchange membrane. Likewise, the negatively charged anions move to the anode, passing through the anion exchange membrane and retained by the cation exchange membrane (Kabay et al. 2008). As a result, ion concentration increases in alternate compartments with a simultaneous decrease of ion concentration in other compartments (Sadrzadeh & Mohammadi 2008).

Due to the high selectivity and low chemical demand, ED system has been proved to be a reliable and efficient method for both of the desalination and the selective removal such as fluoride and nitrate (Banasiak et al. 2007). However, due to its high operating costs, ED might not be the best appropriate technology for the ion removal (Banasiak et al. 2007). Therefore, the development of ion-exchange membranes have gained further interests for better selectivity, improved chemical and mechanical properties, and lower electrical resistance (Helfferich 2005).

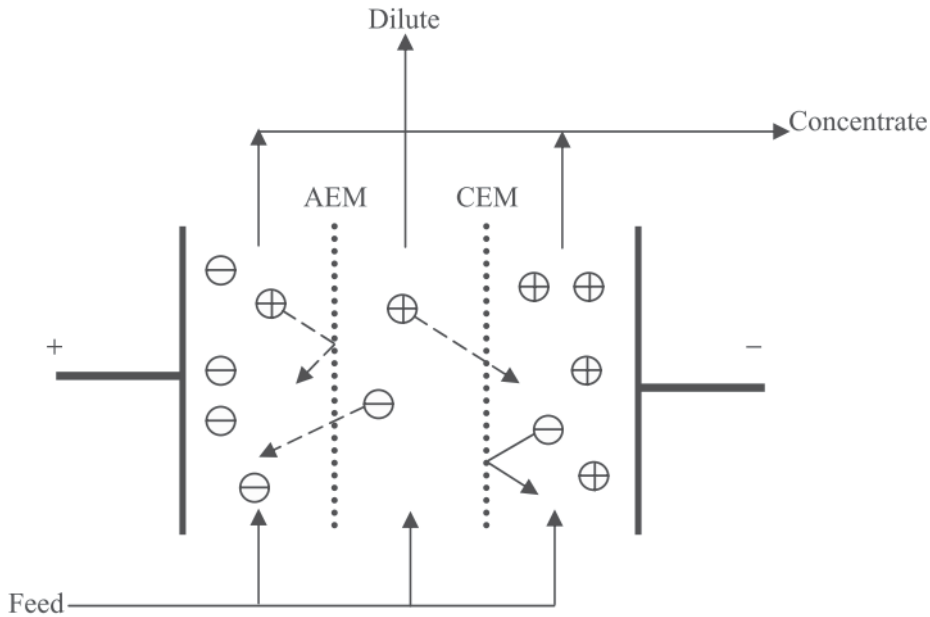

Figure 2. Schematic view of an electrodialysis (ED) cell (Sadrzadeh & Mohammadi 2008).

2.3 Fluoride Selective Materials

2.3.1 Hydroxyapatite

Hydroxyapatite ($Ca_{10}(PO_4)_6(OH)_2$) (HA) has been proved as the most effective adsorbent for the fluoride removal with its low cost, availability, and high defluoridation capacity (Yu et al. 2013). It has a unique hexagonal crystal structure, consisting of two different calcium sites, phosphorous site, and hydroxyl site (Figure 3). According to several research done for the fluoride removal with HA adsorbent, it has been found that the mechanism of the fluoride adsorption is due to electrostatic attractions and ion exchange processes (Medellin-Castillo et al. 2014).

With its high ion adsorption performance and large surface site, n-HA (nanoscale HA) is widely used in the process of water treatment. For instance, there are several studies reported for removing heavy metals such as cadmium, oxovanadium, cobalt, lead and zinc using HA (Lusvardi et al., 2002, Vega et al., 2003, Smičiklas et al., 2006, Sandrine et al., 2007, Sheha, 2007). It was investigated that the adsorption of Pb^{2+}, Cu^{2+} and Cd^{2+} from aqueous solutions to HA has been attributed to the ion exchange of Ca^{2+} on the HA by the metal cation in solution (Kofa et al. 2017). n-HA has been synthesized by various ceramic processes including precipitation, sol-gel, and hydrothermal processing (Sundaram et al. 2008). Moreover, several properties of HA have gained large research attentions in the last two decades such as its structure, ion exchange capacity, adsorption affinity, and capacity to bind with organic molecules of different sizes.

Along with various research studies, adsorption of the fluoride on the HA has also been reported in several works (Murray et al. 1995). For instance, Sundaram et al (Sundaram et al. 2008) synthesized n-HA by precipitation and used it to remove the fluoride from aqueous solution with the adsorption capacity of 1.457 mg g^{-1}. Gao et al (Gao et al. 2009) also prepared an n-HA by the decomposition of precursor and then investigated the defluoridation ability. It was found that the adsorption capacity of fluoride could reach up to 0.489 mg g^{-1}. However, due to the high specific surface area of the nanoscale HA, the agglomeration was a critical concern, leading to the low adsorption capacity of fluoride. Accordingly, there have been several approaches making a composite with template material such as cellulose (Yu et al. 2013) or chitosan (Sairam Sundaram et al. 2008) to overcome the agglomeration of nanoscale n-HA.

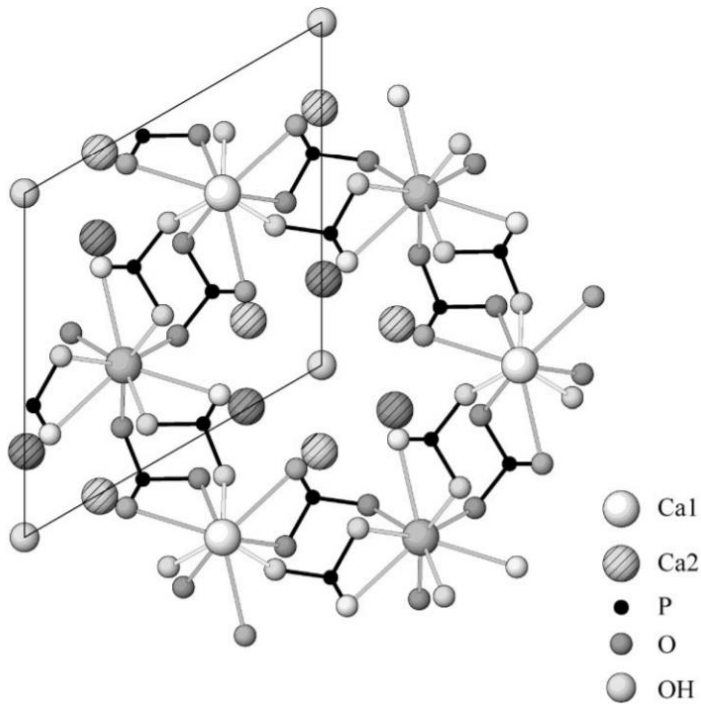

Figure 3. Crystal structure of hydroxyapatite. Projection onto the (0001) plane (Ivanova et al. 2001).

2.3.2 Resin

Ion exchangers are proved to be one of the most promising materials in the domain of water treatment with its selectivity for specific ion and high capacity. There have been several studies for the fluoride adsorption with various ion-exchange resins such as metal-loaded amberlite resin (Luo & Inoue 2004), modified amberlite resin (Solangi et al. 2009), and chelating resin (anion-exchange resin) (Meenakshi & Viswanathan 2007). Recently, several research have been carried out to remove fluoride using chelating resins loaded with high-valence metals such as iron (III), lanthanum (III), cerium (IV), and zirconium (IV) (Luo & Inoue 2004). With these anion-exchange resins, high fluoride removal efficiency (90-95%) can be achieved. However, due to the problems of high chloride levels in treated water with its chemical use demand and high operational costs, ion exchange resin still has limitation to be applied to the industry.

Chapter 3. Materials and Method

3.1 Material Synthesis

3.1.1 Preparation of rGO/HA composite

rGO/HA was prepared with the hydrothermal method referring to the previous study (Fan et al. 2014). The 282 mg of $Ca(NO_3) \cdot 4H_2O$ (Sigma-Aldrich, United States) was added into 36 mL of Graphene Oxide Solution (5 g L^{-1}, Grapheneall Co., Ltd.) with 54 mL of the distilled water. After the mixture went through the ultrasonication process for 60 min, 120 mg of Cetyltrimethylammonium bromide (CTAB, Fisher Scientific, U.K.) was added into the solution. The solution was sonicated for 60 min to form solution A. Then 309.6 mg of trisodium citrate (Sigma-Aldrich, United States) and 94.68 mg of $(NH_4)_2HPO_4$ (Sigma-Aldrich, United States) were added into 45 mL of ultrapure water to form solution B. Solution B was combined with solution A. This mixed solution was sonicated for 30 min and then moved into a hydrothermal synthesis reactor (150 mL, IN-HP 100, PPL Liner Included). After sealed, the reactor was maintained at 180℃ for 24 h. Then powder-like rGO/HA composite was achieved by the micropore filtration. The composite was washed several times with ethanol and distilled water for complete removing of CTAB and trisodium citrate. The composite was then dried at 40℃ for 24 h. From this work, the rGO/HA composite with 48 wt.% of HA was synthesized. For comparison, other rGO/HA composites with 37 and 91 wt.% of HA were also synthesized by changing the concentration of reagents to half and double, excepts

GO solution. rGO and HA were synthesized by the same hydrothermal method with each source reagents.

3.2 Characterization of Materials

The synthesized HA, rGO, and rGO/HA composite powders were visualized by a Field Emission Transmission Electron Microscope (FE-TEM, JEM-F200, JEOL Ltd, Japan). The crystalline structure of the rGO and rGO/HA were probed by the X-ray diffraction (XRD, SmartLab) with 40 kV, 30 mA radiation. The HA contents in the rGO/HA composites were quantified via the elemental analyzer (EA, TruSpec® Micro CHNS). Elemental surface analysis was carried out with the X-ray Photoelectron Spectroscopy (XPS, Sigma probe) to investigate the fluoride adsorption on the surface of the rGO/HA electrode.

The Cyclic voltammetry (CV) was measured by a potentiostat/galvanostat device (PARSTAT 2273, Princeton Applied Research) using a three-electrode cell with a working electrode (HA or rGO/HA), counter electrode (AC) and a reference electrode (Ag/AgCl electrode, sat'd KCl). The scan rate was 1 mV s^{-1} in a 0.5 M single solution of NaF or 3 mM ternary solution of NaF, NaCl, and $NaNO_3$.

The galvanostatic charging/discharging was carried out using a battery cycler (WBCS300, WonA Tech Co, Seoul, Korea) with a reference electrode (Ag/AgCl electrode, sat'd KCl) for monitoring potentials of the rGO/HA electrode.

3.3 Electrode Fabrication and Cell Assembly

3.3.1 Electrode fabrication

The rGO/HA and AC electrodes were prepared as follows: The 80 wt.% of the synthesized rGO/HA or AC (YS-2, Japan Enviro Chemicals, Japan), 10 wt.% of Super P (Timcal, Switzerland), and 10 wt.% polytetrafluoroethylene (PTFE, Sigma-Aldrich) were mixed with ethanol (Sigma-Aldrich) to obtain a slurry mixture. After mixing the resulting slurry, it was rolled using a roll press machine to prepare sheet-type electrodes with 300 μm thickness. The fabricated sheet-type electrodes were dried in an oven at 60℃ for 12 h to remove any remaining solvents.

3.3.2 Cell assembly

The schematic diagram of cell assembly for the performance test of the fluoride removal is depicted in Figure 4. The circular-shaped rGO/HA and AC electrodes (diameter, d: 9 mm for both) were used as working electrodes for defluoridation comparison test. Counter electrodes for all cases were AC electrodes (d: 20 mm). Two pieces of nylon were cut into round shapes (d: 25 mm), to use as spacers between the working and the counter electrodes. The cation exchange membrane (CEM, CMX, Neosepta, Japan) was cut into the circular shape (d: 20 mm) and used for separating cations from the rGO/HA electrodes. By using a peristaltic pump (PMP REGLO ICC 4CHNL 12RLR), the flow rate was maintained with 8 mL min^{-1} for a semi-batch system.

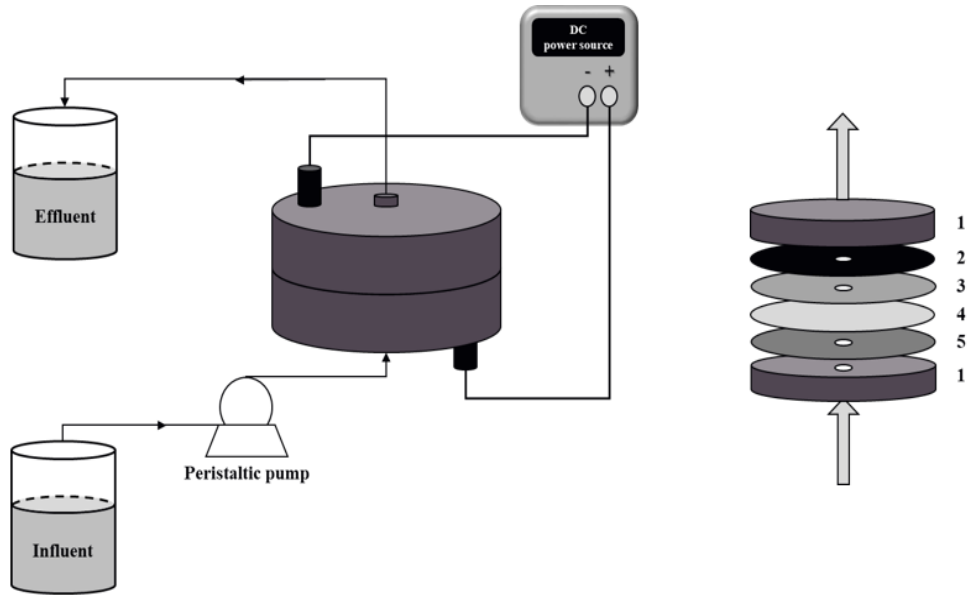

Figure 4. Schematic diagram of cell assembly for fluoride removal performance test (1: current collector, 2: activated carbon electrode, 3: cation exchange membrane, 4: nylon spacer x 2, 5: rGO/HA electrode (or AC for the comparison test))

3.4 Defluoridation Performance Test

The defluoridation performance tests were carried out using the rGO/HA electrode (d: 9 mm) as a working electrode and the AC electrode (d: 20 mm) as a counter electrode. For comparing the selective fluoride uptake, the defluoridation performance test was also conducted using AC electrode as the working electrode. Fluoride removal was proceeded with applying positive voltage to the rGO/HA electrode during 20 min. To demonstrate the fluoride selectivity of the rGO/HA electrode, the ternary solution of NaF, NaCl, and $NaNO_3$ (ternary solution of F^-, Cl^-, and NO_3^-, 1 mM each) was used as feed solution. The fluoride selectivity of the rGO/HA electrode was also verified through the 240 min saturation test with the ternary solution of F^-, Cl^-, and NO_3^-.

To investigate the effect of the electric field on the fluoride removal, various charging voltages (+0.5, +1.2, and +1.5 V) were applied during the adsorption process using an automatic battery cycler (WBC 2000, WonAtech, Korea).

Furthermore, the stability and reusability of the rGO/HA electrode were also evaluated with fluoride adsorption/desorption test before and after 50 cycle operation in the ternary solution of F^-, Cl^-, and NO_3^-. The charging and discharging voltages were +1.2 V and -1.2 V during 20 min, respectively (Figure 5).

Feasibility of the system was also demonstrated in the real groundwater of Mukh Kampul, Cambodia provided by Glory & Tech Co., Ltd. Constant voltages of +1.2 V and -1.2 V were applied for the adsorption and desorption process,

respectively, and the experiments were conducted for three cycles. Along with the system using the rGO/HA electrode, AC electrode was used as the working electrode as a comparison. For the fluoride desorption process, 3 mM of Na_2SO_4 solution was used as a supporting electrolyte.

For overall tests, concentrations of various anion components were evaluated by the ion chromatography (IC, DX-120, DIONEX). Throughout the study, system was operated for 20 min of both adsorption and desorption tests, unless it is mentioned specifically.

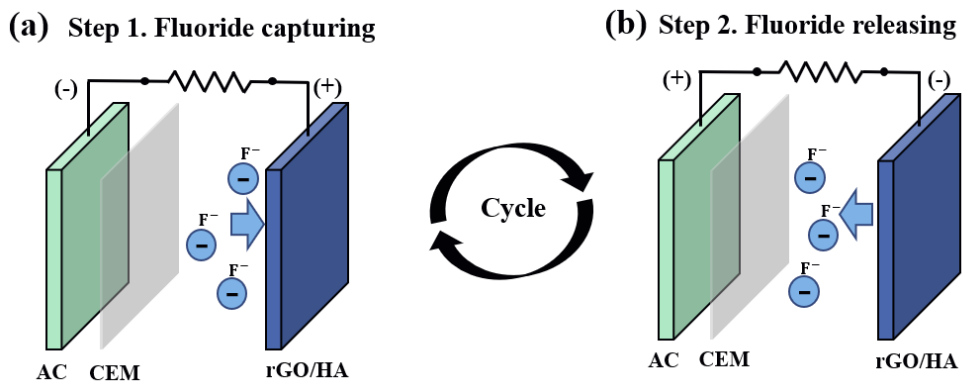

Figure 5. Schematic illustration of fluoride capturing (adsorption) and releasing (desorption) process with the rGO/HA/AC system.

Chapter 4. Results & Discussion

4.1 Characterization of rGO/HA

Figure 6(a-c) indicate the TEM images of the synthesized HA, rGO, and rGO/HA composite, respectively. Figure 6(a) shows the HA particles with nanoscale rod shape. Figure 6(b) presents the rGO of a thin sheet form. Subsequently, Figure 6(c) shows the considerable amounts of nanoscale rods spreading on the sheet, which indicates the HA particles synthesized on the rGO. Figure 6(d) represents the XRD patterns of synthesized rGO, HA and a typical pattern of the HA. Several identical peaks of the HA were detected in the XRD patterns of the rGO/HA, indicating that the synthesized rGO/HA composite involves HA properties. Through the TEM images and the XRD patterns, it can be explained that the rGO/HA composite was successfully synthesized.

Figure 7(a) depicts the cyclic voltammograms of the HA electrode and the rGO/HA electrode (with 48 wt.% of HA) in the single solution of F^- (0.5 M). The rGO/HA electrode (76 F g^{-1}) shows about 77 times larger specific capacity than the HA electrode (0.95 F g^{-1}) within the potential range from -1 V to 1 V (vs. Ag/AgCl). This result proves that the rGO conductive properties can contribute the conductivity to the HA through synthesizing. The rGO helps to form an electric field, increasing the fluoride concentration near the electrode; thus, the HA could adsorb fluoride more effectively. Figure 7(b) reveals the cyclic voltammograms of the rGO/HA electrodes with different wt.% of HA in the ternary solution of F^-, Cl^-, and NO_3^- (1

mM each). According to Figure7(b), the rGO/HA composite with 48 wt.% of HA (36 F g^{-1}) reveals 1.4 times higher capacity than with 91 wt.% of HA (26 F g^{-1}) and even 4.9 times higher capacity that with 38 wt.% of HA (7.3 F g^{-1}). In this regard, it seems that the HA gain the highest conductive property with 48 wt.% of HA; for this reason, the rGO/HA composite with 48 wt.% of HA was used for further studies.

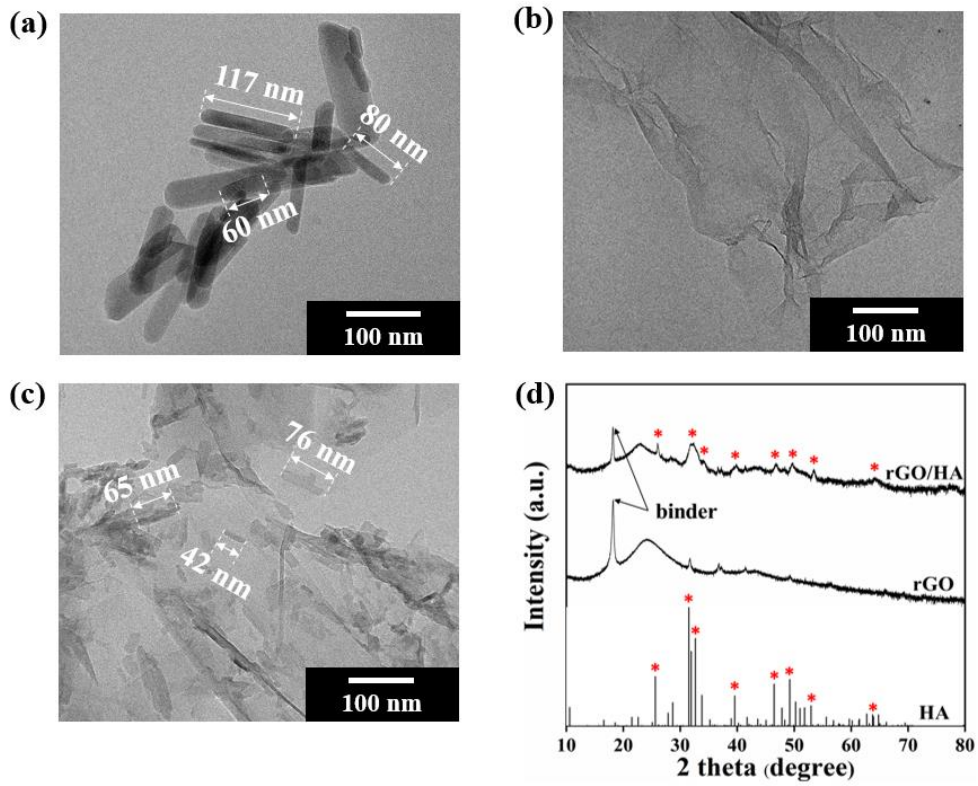

Figure 6. (a-c) TEM images for the synthesized HA, rGO, and rGO/HA composite, (d) XRD patterns of the synthesized rGO/HA, rGO, and a typical pattern of HA.

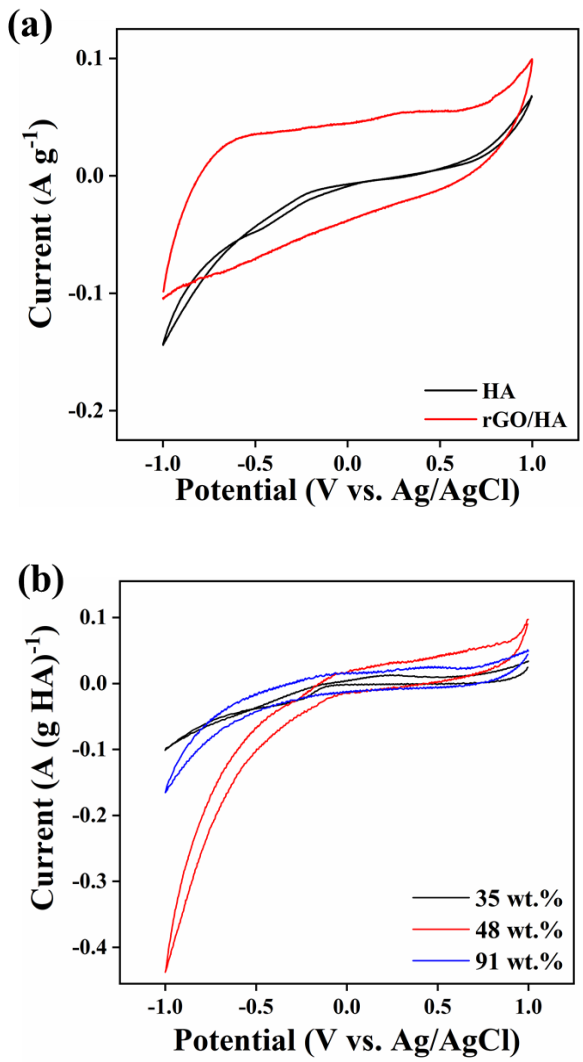

Figure 7. Cyclic voltammograms of (a) the HA electrode and the rGO/HA electrode in the single solution of F^- (0.5 M), and that of (b) the rGO/HA electrodes with different wt.% of HA in the ternary solution of F^-, Cl^-, and NO_3^- (1 mM each). Both cyclic voltammograms were operated with 1 mV s^{-1} of the scan rate.

4.2 Selective Fluoride Removal Properties

Figure 8(a) shows the fluoride uptake in the single solution of F^- (1 mM) and the ternary solution of F^-, Cl^-, and NO_3^- (1 mM each) with the AC electrode and the rGO/HA electrode. When the feed solution changed from the single solution of F^- to the ternary solution of F^-, Cl^-, and NO_3^-, the fluoride removal capacity of the AC electrode dramatically decreased from 0.21 mmol g^{-1} to 0.041 mmol g^{-1}, which is approximately 80% of reduction. However, compared to the AC electrode, the rGO/HA electrode shows a slight increase of the fluoride removal capacity with the solution change from the single to the ternary solution, indicating 0.14 mmol g^{-1} and 0.20 mmol g^{-1}, and this can be explained by the solution resistance decrease with concentration increase.

Figure 8(b) exhibits the anion concentration change profile with respect to time for the rGO/HA electrode in the ternary solution of F^-, Cl^-, and NO_3^- (1 mM each) during 1.2 V fluoride adsorption process. The efficiency of the fluoride removal at adsorption equilibrium was 18%, whereas that of chloride and nitrate removal were 6.9% and 7.6%, respectively, indicating more than twice less value. From these results, it can be examined that the rGO/HA electrode has exceptional fluoride selective properties and high capacity, providing the feasibility of the rGO/HA electrode in the fluoride removal in the electric field system.

Figure 9 indicates the fluoride removal capacity at various wt.% of HA in the rGO/HA electrode. It shows that the fluoride removal capacities were 0.16, 0.19,

and 0.24 mmol g^{-1} for 35, 48, and 91 wt.% of HA, respectively. These results indicate that synthesizing HA to rGO can enhanced the fluoride removal capacity up to 11 times more than that of the rGO electrode (0.022 mg g^{-1}). Through the positive relation between the fluoride removal capacity and the HA wt. % of the rGO/HA electrode, it can be suggested that the HA ratio is mainly related to the fluoride removal of the rGO/HA electrode. Therefore, HA synthesizing can attribute to achieve high fluoride removal capacity, giving a potential of HA application to supporting materials for fluoride removal.

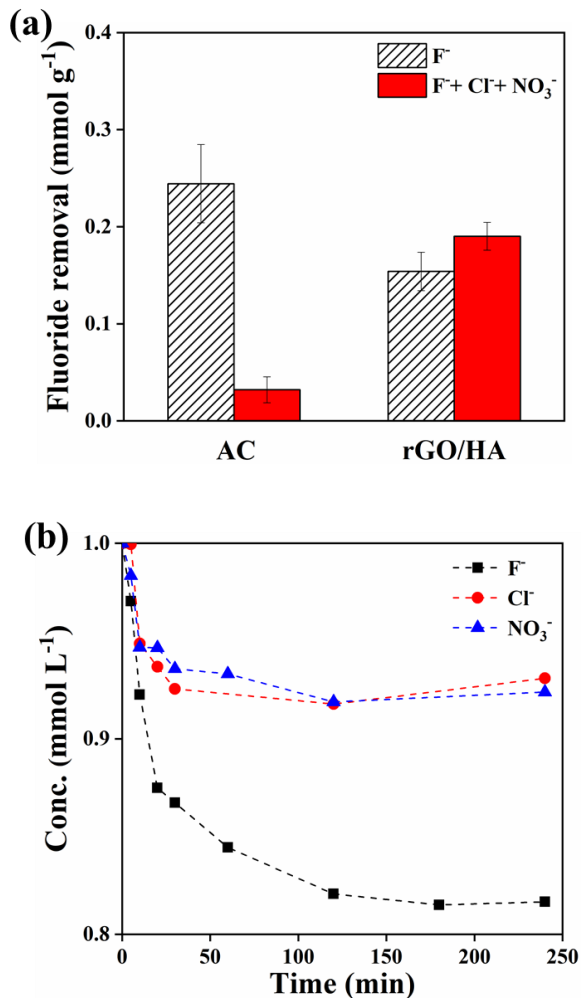

Figure 8. (a) Fluoride removal capacity in the single solution of F^- (1mM) and the ternary solution of F^-, Cl^-, and NO_3^- (1 mM each) with the AC electrode and the rGO/HA electrode (V_{ads}=1.2 V, t_{ads}=20 min), (b) Anion concentration change with respect to time for the fluoride adsorption process with the rGO/HA electrode (V_{ads}=1.2 V, t_{ads}=240 min)

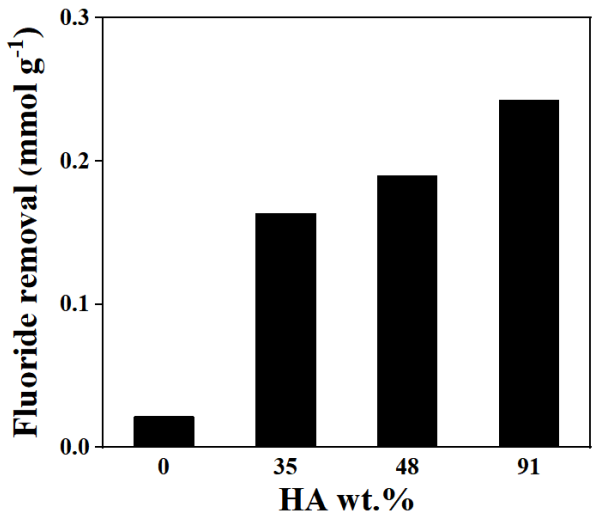

Figure 9. Fluoride removal capacity of the rGO/HA electrodes with different wt.% of HA (V_{ads}=1.2 V, t_{ads}=20 min).

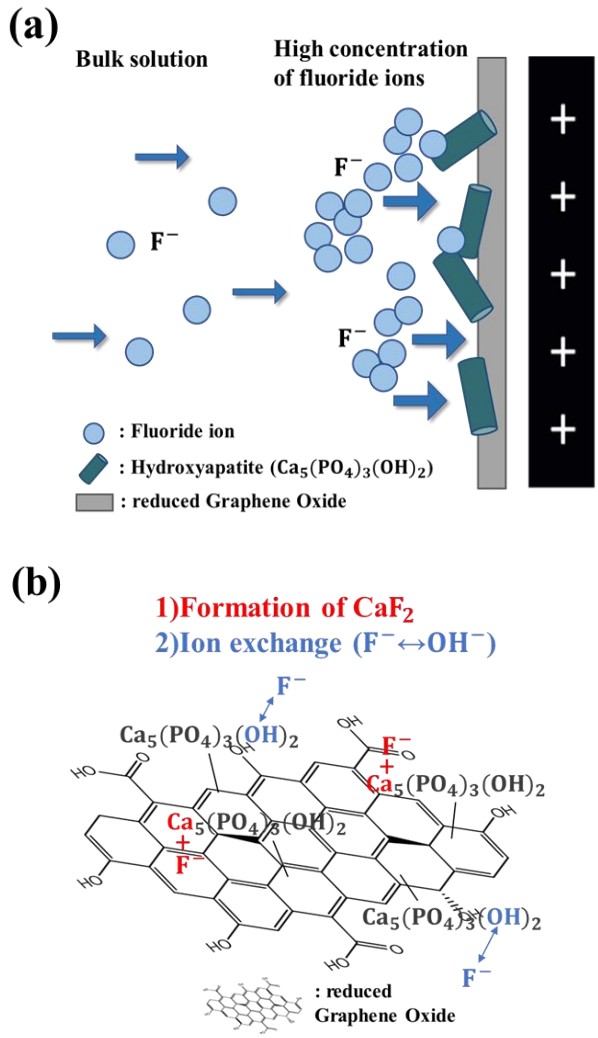

Figure 10. Schematic illustration of (a) the fluoride ion diffusion to the rGO/HA electrode by electric field and (b) the fluoride adsorption principle with the HA on the rGO.

4.3 Electric Field Dependent Fluoride Removal

Figure 11 shows the effect of the electric field on fluoride removal capacity and rate. Figure 11(a) presents the fluoride removal capacity and pH of treated solution with respect to the applied voltages using the rGO/HA electrode. The fluoride removal capacity was 0.11, 0.19, and 0.12 mg g^{-1} at 0.5, 1.2, and 1.5 V applied voltages, respectively. The fluoride removal capacity at 1.2 V (0.19 mg g^{-1}) was 2.4 times higher than that of 0 V (0.078 mg g^{-1}), which was adsorption process without voltage applying. From the results shown, as the applied voltage increased from 0.5 V to 1.2 V, the fluoride removal capacity enhanced from 0.11 mg g^{-1} to 0.19 mg g^{-1}, showing 73% increased capacity. On the other hand, when it comes to 1.5 V, the fluoride removal capacity significantly reduced more than 40% compared to the that of at 1.2 V with pH decrease. It can be explained by the dominant oxygen forming via water electrolysis (Nagai et al. 2003), which leads reduction of the actual conductivity of the electrolyte and following electrochemical resistance and mass transfer barriers to the electrode reactions (Jalali et al., 2009, Zhang and Zeng, 2012). Thus, proper applied voltage is considered to be under 1.2 V, indicating over 1.5 V of applied voltage accompanies considerable decrease of fluoride removal capacity. Furthermore, as shown in Figure 11(b), the fluoride removal rates were enhanced with increasing applied voltages from 0 V to 1.2 V. Similar to the trend of fluoride removal capacity, the fluoride removal rate was also declined at 1.5 V. As the charging voltage applied to the system, fluoride could be enriched near the electrode,

allowing HA to adsorb fluoride rapidly. This implies that the fluoride removal capacity and rate with the rGO/HA electrode are electric field dependent, and the electric field can help to achieve high fluoride removal efficiency as well as fast fluoride removal (Figure 10). From these results, it can be demonstrated that the electric field affects the fluoride removal capacity and fluoride removal rate. However, to enhance the fluoride removal performance, applied voltages in adequate range would be needed.

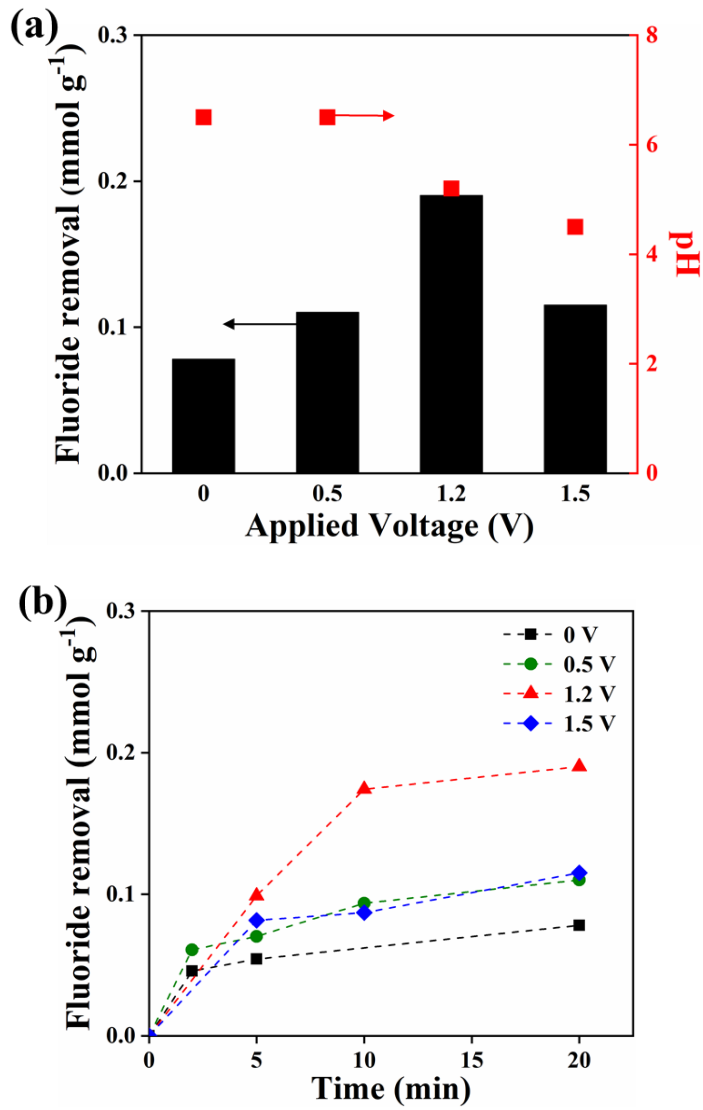

Figure 11. (a) Fluoride removal capacity and pH of the treated solution with respect to different voltages with the rGO/HA electrode (ternary solution of F^-, Cl^-, and NO_3^- (1 mM each), Initial pH = 6, t_{ads}=20 min), (b) Fluoride removal capacity according time with different voltage applying to the rGO/HA electrode (ternary solution of F^-, Cl^-, and NO_3^- (1 mM each)).

4.4 Operation Stability and Chemical Free Regeneration

Figure 12 shows the fluoride adsorption/desorption capacities with regeneration efficiencies at initial and after 50 cycles operation, respectively. There was no significant difference between adsorption and desorption capacity at initial (0.19 mmol g^{-1} and 0.19 mmol g^{-1}) and after 50 cycles (0.21 mmol g^{-1} and 0.20 mmol g^{-1}), respectively. Furthermore, regeneration efficiencies at initial and after 50 cycles were similar with about 96%. The capacitive current in the rGO/HA electrode from the galvanostatic charging/discharging curves (Figure 13) can supports the regeneration possibility of this electrode, showing current flows in the electrode during the regeneration step. Hence, it can be said that the rGO/HA electrode has exceptional regeneration efficiency with high stability even after considerable cyclic operation.

Besides, the electric field assisted system using the rGO/HA electrode is an environmentally benign technology without using any chemicals during fluoride desorption process. Table 3 exhibits chemicals needed for fluoride desorption with conventional fluoride adsorbents. Fluoride adsorbents require high concentration of strong acids such as HCl or bases such as NaOH for fluoride desorption or, which are very toxic and harmful for the environment. However, since the rGO/HA electrode works in the electric field assisted system, toxic chemicals are unnecessary for the fluoride desorption. This suggests that the rGO/HA electrode can achieve a sustainable defluoridation in an environmentally benign way.

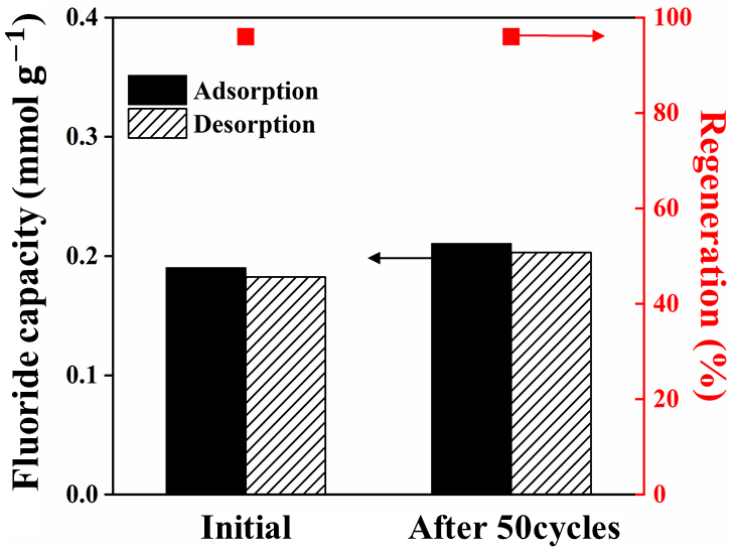

Figure 12. Capacity for fluoride adsorption/desorption and following regeneration efficiency with the rGO/HA electrode at initial and after 50cycles operation (ternary solution of F^-, Cl^-, and NO_3^- (1 mM each), t_{ads}, t_{des} =20 min).

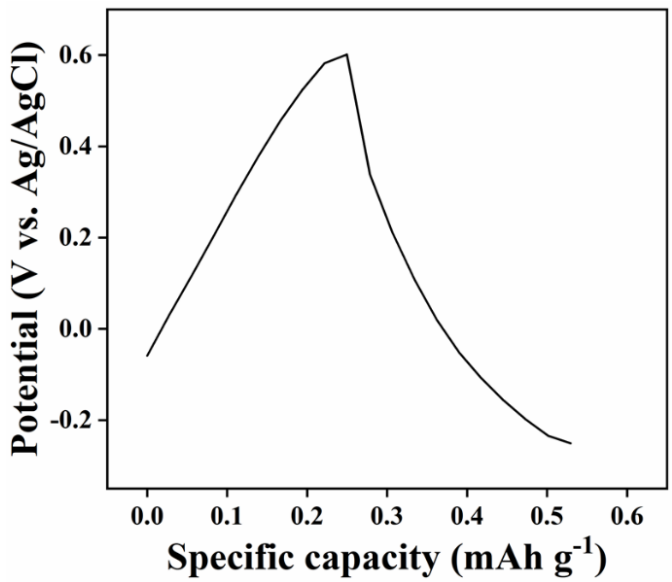

Figure 13. Galvanostatic charge/discharge curve of the rGO/HA electrode in a single solution of F^- (0.5 M).

Table 3. Chemicals needed for fluoride desorption of conventional fluoride adsorbents.

	Chemicals for desorption	Reference
Activated alumina	HCl (0.1 M), NaOH (0.1 M)	(Tripathy et al. 2006)
Chitosan beads	HCl (0.1 M), NaOH (0.1 M), H_2SO_4 (0.1 M)	(Viswanathan et al. 2009)
Amberlite resin	HCl (10%)	(Solangi et al. 2009)
Carbon slurry	HNO_3 (0.1 M), NaOH (0.1 M)	(Gupta et al. 2007)
Granular red mud	NaOH (0.2 M)	(Tor et al. 2009)

4.5 Applying in Real Water

To investigate the applicability of the rGO/HA electrode to remove fluoride in real groundwater, the fluoride adsorption test was conducted in the groundwater sample collected from Mukh Kampul, Cambodia. The initial compositions and their concentrations in this groundwater were listed in Table 4. Figure 14 shows the change in the fluoride concentration over the operating cycles with the AC electrode and the rGO/HA electrode. With the rGO/HA electrode, the fluoride concentration dropped gradually from 2.4 mg L^{-1} to 0.72 mg L^{-1} with operating 3 cycles of adsorption/desorption process. Moreover, it could successfully achieve the fluoride level below the WHO standard of drinking water (1.5 mg L^{-1}) at the 2nd cycle. However, with the AC electrode, the fluoride concentration reduced only to 2.2 mg L^{-1} even after 3 cycles operation which was far greater than the acceptable concentration of the fluoride. With these results, it can be elucidated that the rGO/HA electrode could efficiently remove the fluoride up to the acceptable level for the potable water. Thus, this system could be considered as a promising fluoride removal technology with further studies.

Table 4. The various anion concentrations in real groundwater (Mukh Kampul, Cambodia).

	F^-	Cl^-	$NO_3{}^-$	$SO_4{}^{2-}$	pH
Concentration (mg L^{-1})	2.4	22	1.2	< 1	7.6

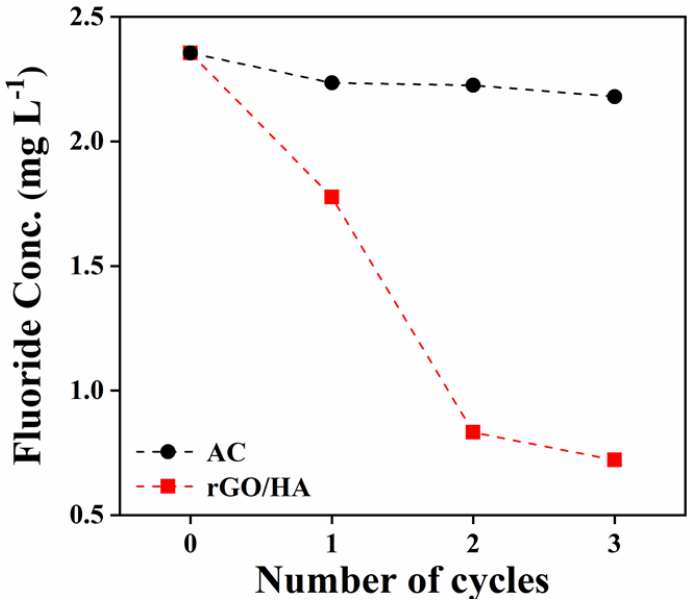

Figure 14. Fluoride concentration change according to the operating cycles with the rGO/HA electrode and the AC electrode in real groundwater (Mukh Kampul, Cambodia).

Chapter 5. Conclusion

In this work, the reduced graphene oxide/hydroxyapatite composite (rGO/HA) was successfully synthesized using reduced graphene oxide (rGO) as a conducting agent and hydroxyapatite (HA) for selective removal of fluoride. The rGO/HA electrode exhibited superior defluoridation performance compared to the AC electrode. With the rGO/HA electrode, F^- in the ternary solution of F^-, Cl^-, and NO_3^- was selectively removed about 5 times higher than that of the AC electrode. Through the positive relationship between the fluoride uptake and the HA content in the rGO/HA electrode as well as applied voltage, it was approved that the HA and applied voltage affect to the enhancement of the fluoride removal capacity. The rGO/HA electrode also showed high stability over 50 cycles, with the negligible capacity loss for both adsorption and desorption processes. Furthermore, the rGO/HA electrode could remove the fluoride in the real groundwater much more efficiently than the AC electrode reaching the WHO standard, showing the feasibility for real industry application. From this study, the system using ion-selective electrode material is expected to be developed and further applied to various desalination technologies.

References

Ali S, Thakur SK, Sarkar A, Shekhar S. 2016. Worldwide contamination of water by fluoride. *Environ. Chem. Lett.* 14(3):291–315

Banasiak LJ, Kruttschnitt TW, Schäfer AI. 2007. Desalination using electrodialysis as a function of voltage and salt concentration. *Desalination*. 205(1–3):38–46

Bhatnagar A, Kumar E, Sillanpää M. 2011. Fluoride removal from water by adsorption-A review. *Chemical Engineering Journal.* 171:811-840

Choi J, Lee H, Hong S. 2016. Capacitive deionization (CDI) integrated with monovalent cation selective membrane for producing divalent cation-rich solution. *Desalination*. 400:38-46

Fan Z, Wang J, Wang Z, Ran H, Li Y, et al. 2014. One-pot synthesis of graphene/hydroxyapatite nanorod composite for tissue engineering. *Carbon N. Y.* 66:407-416

Fordyce FM, Vrana K, Zhovinsky E, Povoroznuk V, Toth G, et al. 2007. A health risk assessment for fluoride in Central Europe. *Environ. Geochem. Health*. 29(2):83–102

Gan L, Wu Y, Song H, Zhang S, Lu C, et al. 2019. Selective removal of nitrate ion using a novel activated carbon composite carbon electrode in capacitive deionization. *Sep. Purif. Technol.* 46(18):728–36

Gao S, Sun R, Wei Z, Zhao H, Li H, Hu F. 2009. Size-dependent defluoridation properties of synthetic hydroxyapatite. *J. Fluor. Chem.*130:550-556

Gupta VK, Ali I, Saini VK. 2007. Defluoridation of wastewaters using waste carbon slurry. *Water Res.* 41(15):3307–16

Helfferich F. 2005. Book review. *Sep. Purif. Technol.* 42(1):101

Indermitte E, Saava A, Karro E. 2014. Reducing exposure to high fluoride drinking water in estonia-a countrywide study. *Int. J. Environ. Res. Public Health*. 11(3):3132–42

Ivanova TI, Frank-Kamenetskaya O V., Kol'tsov AB, Ugolkov VL. 2001. Crystal structure of calcium-deficient carbonated hydroxyapatite. Thermal decomposition. *J. Solid State Chem.* 160(2):340–49

Jadhav S V., Bringas E, Yadav GD, Rathod VK, Ortiz I, Marathe K V. 2015. Arsenic and fluoride contaminated groundwaters: A review of current technologies for contaminants removal. *J. Environ. Manage.* 162:306–25

Jalali AA, Mohammadi F, Ashrafizadeh SN. 2009. Effects of process conditions on cell voltage, current efficiency and voltage balance of a chlor-alkali membrane cell. *Desalination*. 237(1–3):126–39

Kabay N, Arar Ö, Samatya S, Yüksel Ü, Yüksel M. 2008. Separation of fluoride from aqueous solution by electrodialysis: Effect of process parameters and other ionic species. *J. Hazard. Mater.* 153(1–2):107–13

Kim YJ, Choi JH. 2010. Enhanced desalination efficiency in capacitive deionization with an ion-selective membrane. *Sep. Purif. Technol.* 71(1):70–75

Kofa GP, Gomdje VH, Telegang C, Koungou SN. 2017. Removal of Fluoride from Water by Adsorption onto Fired Clay Pots: Kinetics and Equilibrium Studies. *J. Appl. Chem.* 2017:1–7

Luo F, Inoue K. 2004. The removal of fluoride ion by using metal(III)-loaded amberlite resins. *Solvent Extr. Ion Exch.* 22(2):305–22

Lusvardi G, Malavasi G, Menabue L, Saladini M. 2002. Removal of cadmium ion by means of synthetic hydroxyapatite. *Waste Manag.* 22(8):853–57

Malago J. 2017. Fluoride Levels in Surface and Groundwater in Africa: A Review. *Am. J. Water Sci. Eng.* 3(1):1

Medellin-Castillo NA, Leyva-Ramos R, Padilla-Ortega E, Perez RO, Flores-Cano J V., Berber-Mendoza MS. 2014. Adsorption capacity of bone char for removing fluoride from water solution. Role of hydroxyapatite content, adsorption mechanism and competing anions. *J. Ind. Eng. Chem.*20:4014-4021

Meenakshi, Maheshwari RC. 2006. Fluoride in drinking water and its removal. *J. Hazard. Mater.*B137:456-463

Meenakshi S, Viswanathan N. 2007. Identification of selective ion-exchange resin for fluoride sorption. *J. Colloid Interface Sci.* 308(2):438–50

Mesdaghinia A, Vaghefi KA, Montazeri A, Mohebbi MR, Saeedi R. 2010. Monitoring of fluoride in groundwater resources of Iran. *Bull. Environ. Contam. Toxicol.* 84(4):432–37

Murray MGS, Wang J, Ponton CB, Marquis PM. 1995. An improvement in processing of hydroxyapatite ceramics. *J. Mater. Sci.* 30(12):3061–74

Nagai N, Takeuchi M, Kimura T, Oka T. 2003. Existence of optimum space between electrodes on hydrogen production by water electrolysis. *Int. J. Hydrogen Energy*. 28(1):35–41

Ndiaye PI, Moulin P, Dominguez L, Millet JC, Charbit F. 2005. Removal of fluoride

from electronic industrial effluentby RO membrane separation. *Desalination*. 173(1):25–32

Oladoja NA, Aliu YD. 2009. Snail shell as coagulant aid in the alum precipitation of malachite green from aqua system. *J. Hazard. Mater.* 164(2–3):1496–1502

Porada S, Zhao R, Van Der Wal A, Presser V, Biesheuvel PM. 2013. Review on the science and technology of water desalination by capacitive deionization. *Prog. Mater. Sci.* 58(8):1388–1442

Qian B, Wang G, Ling Z, Dong Q, Wu T, et al. 2015. Sulfonated Graphene as Cation-Selective Coating: A New Strategy for High-Performance Membrane Capacitive Deionization. *Adv. Mater. Interfaces*. 2(16):1–9

Sadrzadeh M, Mohammadi T. 2008. Sea water desalination using electrodialysis. *Desalination*. 221(1–3):440–47

Sairam Sundaram C, Viswanathan N, Meenakshi S. 2008. Uptake of fluoride by nano-hydroxyapatite/chitosan, a bioinorganic composite. *Bioresour. Technol.* 99(17):8226–30

Sandrine B, Ange N, Didier BA, Eric C, Patrick S. 2007. Removal of aqueous lead ions by hydroxyapatites: Equilibria and kinetic processes. *J. Hazard. Mater.* 139(3):443–46

Seo SJ, Jeon H, Lee JK, Kim GY, Park D, et al. 2010. Investigation on removal of hardness ions by capacitive deionization (CDI) for water softening applications. *Water Res.*44:2267-2275

Sheha RR. 2007. Sorption behavior of Zn(II) ions on synthesized hydroxyapatites. *J. Colloid Interface Sci.* 310(1):18–26

Shen J, Schäfer A. 2014. Removal of fluoride and uranium by nanofiltration and reverse osmosis: A review. *Chemosphere*. 117(1):679–91

Smičiklas I, Dimović S, Plećaš I, Mitrić M. 2006. Removal of Co 2+ from aqueous solutions by hydroxyapatite. *Water Res.* 40(12):2267–74

Solangi IB, Memon S, Bhanger MI. 2009. Removal of fluoride from aqueous environment by modified Amberlite resin. *J. Hazard. Mater.* 171(1–3):815–19

Sundaram CS, Viswanathan N, Meenakshi S. 2008. Defluoridation chemistry of synthetic hydroxyapatite at nano scale: Equilibrium and kinetic studies. *J. Hazard. Mater.* 155(1–2):206–15

Tang W, Kovalsky P, Cao B, He D, Waite TD. 2016a. Fluoride Removal from Brackish Groundwaters by Constant Current Capacitive Deionization (CDI). *Environ. Sci. Technol.* 50(19):10570–79

Tang W, Kovalsky P, Cao B, Waite TD. 2016b. Investigation of fluoride removal from low-salinity groundwater by single-pass constant-voltage capacitive deionization. *Water Res.* 99:112–21

Tang W, Kovalsky P, He D, Waite TD. 2015. Fluoride and nitrate removal from brackish groundwaters by batch-mode capacitive deionization. *Water Res.* 84:342–49

Tor A, Danaoglu N, Arslan G, Cengeloglu Y. 2009. Removal of fluoride from water by using granular red mud: Batch and column studies. *J. Hazard. Mater.* 164(1):271–78

Tripathy SS, Bersillon JL, Gopal K. 2006. Removal of fluoride from drinking water by adsorption onto alum-impregnated activated alumina. *Sep. Purif. Technol.* 50(3):310–17

Turner BD, Binning P, Stipp SLS. 2005. Fluoride removal by calcite: Evidence for fluorite precipitation and surface adsorption. *Environ. Sci. Technol.* 39(24):9561–68

Vega ED, Pedregosa JC, Narda GE, Morando PJ. 2003. Removal of oxovanadium(IV) from aqueous solutions by using commercial crystalline calcium hydroxyapatite. *Water Res.* 37(8):1776–82

Viswanathan N, Sundaram CS, Meenakshi S. 2009. Removal of fluoride from aqueous solution using protonated chitosan beads. *J. Hazard. Mater.* 161(1):423–30

Yang J, Zou L, Choudhury NR. 2013a. Ion-selective carbon nanotube electrodes in capacitive deionisation. *Electrochim. Acta*.91:11-19

Yang J, Zou L, Choudhury NR. 2013b. Ion-selective carbon nanotube electrodes in capacitive deionisation. *Electrochim. Acta*. 91:11–19

Yu X, Tong S, Ge M, Zuo J. 2013. Removal of fluoride from drinking water by cellulose@hydroxyapatite nanocomposites. *Carbohydr. Polym.* 92(1):269–75

Zhang D, Zeng K. 2012. Evaluating the behavior of electrolytic gas bubbles and their effect on the cell voltage in alkaline water electrolysis. *Ind. Eng. Chem. Res.* 51(42):13825–32

국문 초록

전세계 20 개 이상의 국가에서 식수 과불소화 문제가 증가하고 있으며, 관련하여 수계 불소이온 제거 연구들 또한 다양하게 진행되어 왔다. 그중 축전식 탈염공정 (Capacitive Deionization, CDI)은 활성탄 (Activated Carbon, AC)을 전극물질로 하여 전극 표면의 전기 이중층을 통해 탈염을 진행하는 기술로서 에너지 효율적, 환경 친화적인 특징과 함께 각광받고 있다. 최근 이러한 CDI 를 이용한 불소제거 관련 연구들 또한 이루어져 왔다. 하지만 본 연구들은 불소제거 성능 향상이 아닌 모델링 관련 연구에 제한 되어있고, 사용되는 활성탄 전극은 이온 선택성이 없어 혼합물에서의 표적이온 제거 시 불필요한 에너지 소비를 초래한다는 단점이 있다.

본 연구에서는 불소 흡착제로 알려진 수산화인회석 (Hydroxyapatite, HA)과 전도성을 가진 환원 그래핀옥사이드 (reduced Graphene Oxide, rGO)를 합성한 환원 그래핀옥사이드/수산화인회석 (reduced Graphene Oxide/Hydroxyapatite, rGO/HA) 전극을 통해 전기장 시스템에서의 선택적 불소제거성능을 입증하였다. 불소, 염소, 그리고 질산 이온으로 구성된 혼합용액에서 rGO/HA 전극은 AC 전극 대비 약 4.9 배의 불소제거능을 가지며 훨씬 선택적인 불소제거가 가능하게 하였다. 또한, 전압과 rGO/HA 내의 HA 중량 비율 증가에 따른 불소

제거 실험을 통해 적정 범위내의 전압 및 HA 함량의 증가는 불소제거능 향상에 도움을 준다는 것을 입증하였다. 또한 50 번의 흡/탈착 운전 후의 불소 제거능과 재생 효율은 약 0.21 mmol g^{-1}, 96% 정도로 초기 운전 결과에 비하여 유의미한 감소가 없음을 보여주며, rGO/HA 전극은 불소 제거 시 전극의 안정성 및 재사용성을 갖는 것을 증명하였다. 더 나아가, 실제 원수에서의 흡/탈착 운전 사이클에 따른 불소제거 실험에서 본 전극은 AC 전극보다 훨씬 우수한 불소제거능과 함께 세계보건기구 음용수 불소농도 기준에 도달하며, 실제 산업에서의 적용 가능성 또한 입증하였다. 본 시스템은 전기장 내에서의 선택적 불소제거와 함께 독성 화학물질의 사용없이 재생 가능하고 실제 산업에까지 적용 가능한 환경친화적 시스템을 제안하며, 이와 같은 이온 선택적 전극 합성 및 시스템적용을 활용한 다양한 연구를 통해 이온제거 기술을 더 발전시킬 수 있을 것으로 예상된다.

주요어: 수처리, 선택적 불소제거, 환원그래핀옥사이드/수산화인회석 화합물 전극, 전기장 시스템

학번: 2018-20123